

EFFECT OF SUBSTRATE TEMPERATURE ON THE MORPHOLOGY AND CRYSTALLINITY OF TiO₂ THIN FILMS GROWN BY ALD USING TTIP AND H₂O

✉Temur K. Turdaliev*, Khojiakhmad Kh. Zokhidov, ✉Shukhrat Ch. Iskandarov,
✉Usmonjon F. Berdiyev

*Arifov Institute of Ion-Plasma and Laser Technologies of Uzbekistan Academy of Sciences
100125, Durmon yuli st. 33, Tashkent, Uzbekistan*

**Corresponding Author E-mail: turdaliev@iplt.uz*

Received August 7, 2025; revised October 2, 2025; accepted October 10, 2025

This study investigates the influence of substrate temperature on the morphological and structural characteristics of TiO₂ thin films synthesized by thermal atomic layer deposited (ALD) using titanium tetrakisopropoxide and water as precursors. The substrate temperature was varied from 200 to 275°C in 25°C increments. Surface morphology was examined using atomic force microscopy, while the crystalline structure was analyzed by XRD and Raman spectroscopy. It was found that films deposited at 200 °C exhibited an amorphous structure and a smooth, conformal surface with minimal roughness. Increasing the temperature to 225 °C led to the formation of microstructures and the emergence of initial signs of crystallization, accompanied by an increase in surface roughness. At 250-275 °C, a well-defined polycrystalline anatase structure was formed, characterized by grain development and nanostructure agglomeration, as evidenced by the increased intensity of diffraction peaks and higher surface roughness parameters. According to the XRD analysis, the average crystallite size ranged from 32 to 71 nm, depending on the synthesis temperature. The results demonstrate that deposition temperature exerts a comprehensive effect on both the phase composition and surface morphology of TiO₂ films, which must be considered for their application in functional nanostructures, photocatalytic systems, sensors, and microelectronic devices.

Keywords: TiO₂; ALD; Anatase; Crystallinity; Morphology; Substrate temperature; XRD; Raman

PACS: 81.07.Bc, 81.15.Gh, 68.37.Ps, 61.05.C-

INTRODUCTION

TiO₂ is one of the most extensively studied oxide materials due to its high thermal and chemical stability, environmental safety, and the diversity of its structural modifications. It is widely employed as a functional material in micro- and nanoelectronics, sensing technologies, photocatalysis, as well as in buffer and protective layers within multilayered heterostructures [1,2,3]. Of particular interest is the ability to deliberately control the surface morphology and structural state of TiO₂ thin films, as these characteristics directly influence the material's mechanical, electrical, and diffusion properties [4,5]. The type of crystalline phase, such as anatase, rutile, or brookite, along with crystallite size and orientation, the presence of amorphous components, and surface topography, collectively determine the performance of the film in practical applications [6]. Among the modern techniques for TiO₂ thin film fabrication, ALD stands out as one of the most precise and controllable methods, capable of producing highly uniform coatings even on substrates with complex geometries [7,8].

ALD enables angstrom-level control over film thickness, uniformity, and conformality, making it particularly attractive for the fabrication of nanostructured materials, especially on substrates with complex geometries [9]. In the synthesis of TiO₂ thin films via ALD, various titanium-containing precursors are commonly employed, such as titanium tetrachloride [10], tetrakis(dimethylamido)titanium [11], and titanium tetrakisopropoxide (TTIP) [12], in combination with oxidizing agents like water, oxygen, or ozone. Among these, the thermal ALD process using TTIP and water as precursors is especially advantageous due to its low toxicity, high process stability, and the absence of corrosive by-products such as hydrochloric acid, which are typically generated when using chloride-based precursors [13]. This approach ensures high chemical purity of the resulting films and offers precise control over their thickness and phase composition, which is essential for tailoring the structural and functional properties of TiO₂ layers. One of the most critical parameters in the ALD process is the substrate temperature, which has a pronounced effect on growth mechanisms, the degree of crystallinity, and the surface morphology of the resulting films. At low deposition temperatures, films typically remain amorphous, whereas elevated temperatures can induce crystallization, surface roughening, grain growth, and, beyond the optimal range, agglomeration and loss of uniformity [14].

This work aims to investigate the effect of substrate temperature on the formation of surface morphology and crystalline structure of TiO₂ thin films synthesized by thermal ALD using TTIP and water as precursors. Particular attention is given to the analysis of surface evolution and crystallinity as a function of deposition temperature in the range of 200 - 275°C with 25°C increments, using atomic force microscopy, XRD, and Raman spectroscopy.

EXPERIMENT

TiO₂ thin films were deposited by thermal ALD using an SI PEALD system (SENTECH Instruments GmbH, Germany). Polished monocrystalline silicon wafers with a thickness of 0.4 mm, p-type conductivity, and (100)

crystallographic orientation were used as substrates. TTIP served as the metalorganic precursor, while deionized water was employed as the oxidizing agent. Nitrogen was used as both the carrier and purge gas. The substrate temperature was varied from 200 to 275 °C in 25 °C increments to investigate its effect on the morphology and crystallinity of the resulting films. All other deposition parameters were kept constant and corresponded to previously optimized conditions [12]: nitrogen flow rate of 120 cm³/min, chamber pressure of approximately 60 Pa, and a total cycle duration of 8 s. Each deposition cycle included five steps carried out in sequence: an initial purge with nitrogen, injection of the TTIP precursor for 0.5 s, a nitrogen purge for 3 s, introduction of H₂O for 1.5 s, and a final nitrogen purge for 3 s. The deposition was carried out for 500 cycles under the conditions described above.

The structural properties of the films were investigated using a Renishaw InVia Raman spectrometer operating in the visible range with a laser wavelength of $\lambda = 532$ nm. Phase analysis of the samples was performed by XRD using a Rigaku SmartLab diffractometer equipped with a copper anode (Cu K α , $\lambda = 1.5406$ Å). Diffraction data were collected in the 2 θ range from 20° to 75° with a step size of 0.02°. The resulting diffraction patterns were analyzed using the ICSD (Inorganic Crystal Structure Database) to identify the crystalline phases. Surface morphology of the synthesized TiO₂ films was examined by AFM using an AFM-NT MDT Solver Next system operating in contact mode.

Surface Morphology

Surface scanning was performed over areas of 5×5 μm^2 for each deposition temperature. Both two-dimensional topographic images and cross-sectional surface profiles were analyzed, enabling assessment of the influence of substrate temperature on surface relief evolution.

Topographic AFM images of the films deposited at temperatures ranging from 200 to 275 °C are presented in Figure 1(a). A progressive transformation of the surface structure is observed with increasing deposition temperature. At 200 °C, the surface is nearly flat and featureless, indicating a conformal growth mode. At 225 °C, isolated microstructures appear, likely associated with the onset of crystallization and the formation of initial growth centers. At 250 °C, these microstructures become more pronounced and well-defined, suggesting intensified crystallization and the emergence of crystalline phase regions. At 275 °C, a substantial morphological transformation is observed, with the formation of agglomerated spherical nanostructures exhibiting particle sizes of 50-100 nm and an overall cluster diameter of approximately 0.5 μm . This indicates that the upper limit of the optimal ALD process window may have been exceeded, resulting in enhanced surface diffusion and aggregation due to precursor molecule desorption and re-adsorption. Analysis of the surface profiles extracted from the AFM scans is presented in Figure 1(b).

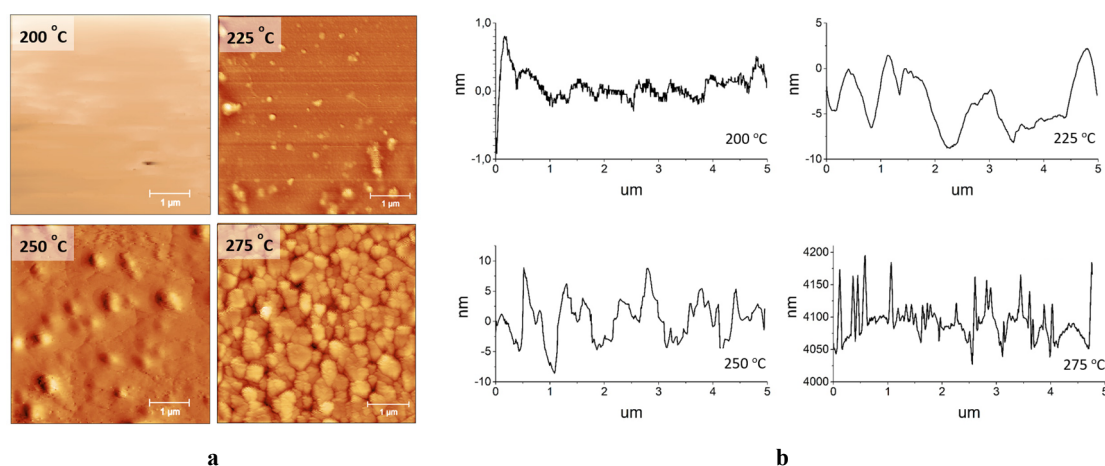


Figure 1. AFM images (a) and cross-sectional profiles (b) of TiO₂ films deposited at 200-275 °C

Quantitative analysis of the AFM surface profiles enabled the determination of key roughness parameters, which are summarized in Table 1. The values of surface roughness and maximum height difference were calculated using standard formulas commonly applied in the interpretation of AFM data.

Table 1. Surface roughness parameters of TiO₂ films deposited at different substrate temperatures

	200 °C	225 °C	250 °C	275 °C
R_a	0.14 nm	2.4 nm	2.69 nm	18.64 nm
R_z	1.73 nm	10.97 nm	17.44 nm	167.92 nm

At 200 °C, the R_a was measured to be 0.14 nm, indicating a highly smooth surface and uniform growth without the formation of local clusters. The film growth at this temperature was predominantly governed by saturated surface reactions. At 225 °C, an increase in surface roughness to 2.40 nm was observed, along with the appearance of microstructures, suggesting the onset of conformality loss and the emergence of crystallization centers. This trend continued at 250 °C, where R_a reached 2.69 nm and R_z was 17.44 nm, reflecting the development of grains and the intensification of grain boundaries. The most significant changes were observed at 275 °C, where R_a increased to 18.64 nm

and R_z to 167.92 nm. These values indicate the formation of a coarse-grained agglomerated structure and a pronounced loss of growth uniformity, likely due to the exceedance of the ALD process temperature window and enhanced thermally driven diffusion processes.

Structural Analysis

The Raman spectrum of the investigated sample exhibits well-defined peaks at 143, 194, 392, and 637 cm⁻¹, along with an intense band at 520 cm⁻¹ (Figure 2). Peak identification was performed based on factor group analysis and comparison with literature data. It is well established that anatase phase TiO₂ exhibits six Raman active modes with symmetries A_{1g}, B_{1g}, and E_g, typically observed at 144, 194, 397, 513, 517, and 639 cm⁻¹ [15]. The peaks recorded at 143, 194, and 637 cm⁻¹ correspond to phonon modes with E_g symmetry, while the band at 392 cm⁻¹ is assigned to the B_{1g} mode. The strong signal at 520 cm⁻¹ originates from Si-Si vibrations and is attributed to the monocrystalline silicon substrate [16]. This substrate-related peak overlaps with the anatase-related A_{1g} and B_{2g} modes at 513 and 517 cm⁻¹, respectively, hindering their unambiguous identification. The rutile phase of TiO₂ is characterized by principal Raman modes at 144, 243, 447, and 612 cm⁻¹ [17]. None of which was observed in the acquired spectrum. Similarly, no bands corresponding to brookite—typically found at 153, 247, 322, 366, 398, 414, and 632 cm⁻¹—were detected [18]. This indicates the absence of both rutile and brookite phases in the film.

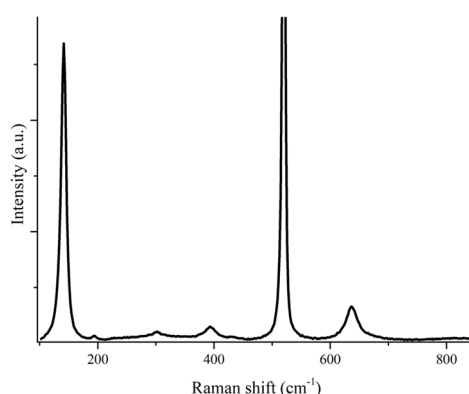


Figure 2. Raman scattering spectrum of the sample

Identification and physical interpretation of the observed Raman peaks: The peak at 143 cm⁻¹ is the most intense and prominent feature of anatase-phase TiO₂. It corresponds to the E_g symmetry phonon mode, associated with symmetric in-plane vibrations of oxygen atoms relative to titanium ions. Its intensity and sharpness are indicative of a high degree of crystallinity and lattice order. The 194 cm⁻¹ peak represents a low-frequency mode with E_g symmetry, attributed to collective oxygen vibrations directed along the crystallographic axis. The 392 cm⁻¹ peak arises from oxygen vibrations perpendicular to the titanium atoms and is characteristic of the B_{1g} mode, reflecting the local symmetry of the anatase crystal lattice. The strong peak at 520 cm⁻¹ originates from the Si-Si bond vibrations of the monocrystalline silicon substrate. In cases of low TiO₂ film thickness, this peak appears as a pronounced background signal, which can mask the intrinsic Raman features of TiO₂, particularly those near 513 and 517 cm⁻¹. The 637 cm⁻¹ peak is a high-frequency mode associated with symmetric oxygen vibrations within the anatase lattice and serves as an additional signature of this crystalline phase. Taken together, the presence and assignment of these peaks confirm that the TiO₂ films synthesized at substrate temperatures of 225–275 °C exhibit a well-defined anatase crystalline structure, while the film grown at 200 °C retains an amorphous phase.

The crystallinity and phase composition of TiO₂ films synthesized at substrate temperatures of 200 °C, 225 °C, 250 °C, and 275 °C were investigated using XRD. In the sample deposited at 200 °C, no diffraction peaks were detected, indicating an amorphous structure with the absence of long-range crystalline order. For the samples synthesized at 225 °C, 250 °C, and 275 °C, the corresponding XRD patterns are shown in Figure 3 (a). At 225 °C, weak but clearly distinguishable diffraction peaks appear, characteristic of the anatase phase of TiO₂. In particular, a peak near $2\theta \approx 25.3^\circ$ corresponds to the (101) crystallographic plane, indicating the initial formation of crystalline nuclei, i.e., growth centers [19]. At the same time, the presence of a broad amorphous background suggests a two-phase composition—comprising both amorphous and crystalline components.

To quantitatively evaluate the phase composition, Rietveld refinement [20] was performed using the reference anatase structure from the ICSD database (entry No. 83795). The analysis revealed that the crystalline phase content in the sample deposited at 225 °C was approximately 25–30%, with the remaining fraction being amorphous. The emergence of crystalline growth centers at this temperature may be attributed to substrate surface characteristics, including morphology, surface energy, and the presence of structural defects that promote localized adsorption and structural ordering. However, crystallization does not extend throughout the entire film, and the majority of the volume remains amorphous.

In contrast, XRD analysis of the samples synthesized at 250 °C and 275 °C revealed sharp and intense diffraction peaks corresponding to the anatase phase of TiO₂. Reflections from the (101), (004), (200), (105), and (211) planes were identified at 2θ angles of approximately 25.3°, 37.8°, 48.0°, and 54.0°, respectively [20]. The presence of narrow and intense peaks indicates a high degree of long-range crystalline order. The absence of a broad amorphous background further confirms the

fully crystallized anatase structure in these films, with no detectable amorphous component. Comparison of the obtained diffraction patterns with the reference anatase phase revealed complete agreement in both peak positions and relative intensities, indicating a polycrystalline anatase structure. The crystallites are randomly oriented, and the diffraction intensity is evenly distributed across all crystallographic directions. Based on the results of XRD and AFM analyses, a schematic representation of the TiO₂ film growth process via ALD at different substrate temperatures is provided in Figure 3(b).

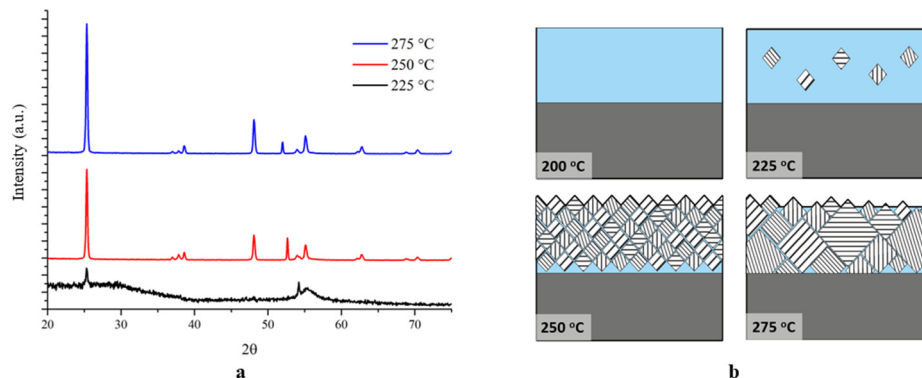


Figure 3. XRD patterns of TiO₂ films (a) and schematic illustration of the temperature-dependent growth mechanism (b)

At 200°C, the film is amorphous, exhibiting a smooth surface with no signs of crystallization. The layer demonstrates high conformality. At 225°C, localized crystallization centers begin to emerge, accompanied by the initial formation of anatase domains. The conformality of the film is partially disrupted. At 250°C, the crystallization process intensifies, resulting in the development of a continuous polycrystalline anatase structure throughout the film. The crystallites are randomly oriented, and the structure appears stabilized. At 275°C, a coarse-grained structure composed of large crystallites is formed. Enhanced surface diffusion results in agglomeration, and the film grows with a loss of uniformity. The average crystallite size was calculated using the Scherrer equation [21]:

$$D = \frac{K\lambda}{\beta \cos \theta}$$

Where D is the average crystallite size, K is the Scherrer constant, λ is the wavelength of Cu K α radiation (0.15406 nm), β is the full width at half maximum (FWHM) of the diffraction peak, and θ is the Bragg angle. For the calculations, five diffraction peaks corresponding to different crystallographic planes were selected, and the FWHM values (β) were measured for each of them. According to the results, the crystallite sizes ranged from 32.2 nm to 71.3 nm, indicating an average crystallite size of approximately 40–70 nm in the investigated TiO₂ samples.

CONCLUSIONS

Structural and morphological characterization of TiO₂ thin films synthesized by thermal ALD using TTIP and H₂O as precursors has demonstrated a strong dependence on substrate temperature. At 200°C, the films exhibit an amorphous structure with conformal surface morphology, as confirmed by the absence of diffraction peaks and a low surface roughness. The onset of crystallization is observed at 225°C, with the emergence of weak diffraction features and microstructural formations, indicating the formation of anatase-phase nuclei. At elevated deposition temperatures of 250–275°C, the TiO₂ films exhibit complete crystallization into the anatase polymorphic phase, as confirmed by the appearance of sharp and intense diffraction peaks corresponding to the (101), (004), (200), and other characteristic crystallographic planes. The crystallite size increases significantly with temperature, reaching ~70 nm, and the films exhibit a coarse-grained polycrystalline structure. AFM analysis reveals a progressive increase in surface roughness, consistent with crystallite growth and agglomeration driven by enhanced surface diffusion. These results confirm that substrate temperature is a critical parameter governing the nucleation, growth mode, and final structural configuration of ALD-deposited TiO₂ films. Control over this parameter enables precise tuning of crystallinity and surface topology, which is essential for optimizing film performance in applications such as photocatalysis, sensors, and nanostructured functional coatings.

Acknowledgments

This research was conducted with the support of budgetary and grant funding from the Academy of Sciences of the Republic of Uzbekistan.

ORCID

©Temur K. Turdaliev, <https://orcid.org/0000-0002-0732-9357>; ©Shukhrat Ch. Iskandarov, <https://orcid.org/0000-0002-3002-9141>
©Usmonjon F. Berdiyev, <https://orcid.org/0000-0003-2808-0105>

REFERENCES

- [1] V. Morgunov, S. Lytovchenko, V. Chyshkala, D. Riabchykov, and D. Matviienko, “Comparison of Anatase and Rutile for Photocatalytic Application: the Short Review,” *East Eur. J. Phys.* (4), 18–30 (2021). <https://doi.org/10.26565/2312-4334-2021-4-02>

- [2] V. Yadav, S. Chaudhary, S.K. Gupta, and A.S. Verma, "Synthesis and characterization of TiO₂ thin film electrode based dye sensitized solar cell," *East Eur. J. Phys.* (3), 129–133 (2020). <https://doi.org/10.26565/2312-4334-2020-3-16>
- [3] Y. Song, J. Yuan, Q. Chen, X. Liu, Y. Zhou, J. Cheng, S. Xiao, M.K. Chen, and Z. Geng, "Three-dimensional varifocal meta-device for augmented reality display," *Photonix*, **6**(1), (2025). <https://doi.org/10.1186/s43074-025-00164-9>
- [4] P.P. Conti, E. Scopel, E.R. Leite, and C.J. Dalmaschio, "Nanostructure morphology influences in electrical properties of titanium dioxide thin films," *J. Mater. Res.* **35**(21), 3012–3020 (2020). <https://doi.org/10.1557/jmr.2020.235>
- [5] E. Kumi-Barimah, R. Penhale-Jones, A. Salimian, H. Upadhyaya, A. Hasnath, and G. Jose, "Phase evolution, morphological, optical and electrical properties of femtosecond pulsed laser deposited TiO₂ thin films," *Sci. Rep.* **10**(1), 1–12 (2020). <https://doi.org/10.1038/s41598-020-67367-x>
- [6] D.A.S. Mulus, M.D. Permana, Y. Deawati, and D.R. Eddy, "A current review of TiO₂ thin films: synthesis and modification effect to the mechanism and photocatalytic activity," *Appl. Surf. Sci. Adv.* **27**, 100746 (2025). <https://doi.org/10.1016/j.apsadv.2025.100746>
- [7] J.P. Niemelä, G. Marin, and M. Karppinen, "Titanium dioxide thin films by atomic layer deposition: A review," *Semicond. Sci. Technol.* **32**(9), 1–20 (2017). <https://doi.org/10.1088/1361-6641/aa78ce>
- [8] J.P. Klesko, R. Rahman, A. Dangerfield, C.E. Nanayakkara, T. L'Esperance, D.F. Moser, L. Fabián Peña, E.C. Mattson, C.L. Dezelah, R.K. Kanjolia, and Y.J. Chabal, "Selective Atomic Layer Deposition Mechanism for Titanium Dioxide Films with (EtCp)Ti(NMe₂)₃: Ozone versus Water," *Chem. Mater.* **30**(3), 970–981 (2018). <https://doi.org/10.1021/acs.chemmater.7b04790>
- [9] T.K. Turdaliev, K.B. Ashurov, and R.K. Ashurov, "Morphology and Optical Characteristics of TiO₂ Nanofilms Grown by Atomic-Layer Deposition on a Macroporous Silicon Substrate," *J. Appl. Spectrosc.* **91**(4), 769–774 (2024). <https://doi.org/10.1007/s10812-024-01783-z>
- [10] L. Aarik, T. Arroval, R. Rammula, H. Mändar, V. Sammelselg, and J. Aarik, "Atomic layer deposition of TiO₂ from TiCl₄ and O₃," *Thin Solid Films* **542**, 100–107 (2013). <https://doi.org/10.1016/j.tsf.2013.06.074>
- [11] J.-J. Park, W.-J. Lee, G.-H. Lee, I.-S. Kim, B.-C. Shin, and S.-G. Yoon, "Very Thin TiO₂ Films Prepared by Plasma Enhanced Atomic Layer Deposition (PEALD)," *Integr. Ferroelectr.* **68**(1), 129–137 (2004). <https://doi.org/10.1080/10584580490895815>
- [12] T.K. Turdaliev, "Optical Performance and Crystal Structure of TiO₂ Thin Film on Glass Substrate Grown by Atomic Layer Deposition," *East Eur. J. Phys.* (1), 250–255 (2025). <https://doi.org/10.26565/2312-4334-2025-1-27>
- [13] C. Armstrong, L.-V. Delumeau, D. Muñoz-Rojas, A. Kursumovic, J. MacManus-Driscoll, and K.P. Musselman, "Tuning the band gap and carrier concentration of titania films grown by spatial atomic layer deposition: a precursor comparison," *Nanoscale Adv.* **3**(20), 5908–5918 (2021). <https://doi.org/10.1039/D1NA00563D>
- [14] N.K. Chowdhary, and T. Gougousi, "Temperature-Dependent Properties of Atomic Layer Deposition-Grown TiO₂ Thin Films," *Adv. Mater. Interfaces* **2400855**, (2025). <https://doi.org/10.1002/admi.202400855>
- [15] A.E. Maftai, A. Buzatu, G. Damian, N. Buzgar, H.G. Dill, and A.I. Apopei, "Micro-Raman—a tool for the heavy mineral analysis of gold placer-type deposits (Pianu Valley, Romania)," *Minerals* **10**(11), 1–17 (2020). <https://doi.org/10.3390/min10110988>
- [16] M. Kadlecíková, L. Vančo, J. Breza, M. Mikolášek, K. Hušková, K. Fröhlich, P. Procel, M. Zeman, and O. Isabella, "Raman spectroscopy of silicon with nanostructured surface," *Optik (Stuttg.)* **257**, 168869 (2022). <https://doi.org/10.1016/j.ijleo.2022.168869>
- [17] T. Lan, X. Tang, and B. Fultz, "Phonon anharmonicity of rutile TiO₂ studied by Raman spectrometry and molecular dynamics simulations," *Phys. Rev. B - Condens. Matter Mater. Phys.* **85**(9), (2012). <https://doi.org/10.1103/PhysRevB.85.094305>
- [18] M.N. Iliev, V.G. Hadjiev, and A.P. Litvinchuk, "Raman and infrared spectra of brookite (TiO₂): Experiment and theory," *Vib. Spectrosc.* **64**, 148–152 (2013). <https://doi.org/10.1016/j.vibspec.2012.08.003>
- [19] S. Prachakiew, S. Boonphan, Y. Keereeta, C. Boonruang, and A. Klinbumrung, "Structural Influence of Vanadium on the Anatase-to-Rutile Phase Transition and Bandgap Modification in TiO₂ Nanocrystals," *Arab. J. Sci. Eng.* (2025). <https://doi.org/10.1007/s13369-025-10150-9>
- [20] M.T. Islam, S. Aman, T. Bayzid, M.A. Rahaman, U. Podder, G.M. Arifuzzaman Khan, and M.A. Alam, "Crystal growth behavior of nanocrystal anatase TiO₂: A Rietveld refinement in WPPF analysis," *Chem. Inorg. Mater.* **6**, 100108 (2025). <https://doi.org/10.1016/j.cinorg.2025.100108>
- [21] T. Theivasanthi, and M. Alagar, "Titanium dioxide (TiO₂) Nanoparticles XRD Analyses: An Insight," *ArXiv:1307.1091*, (2013). <https://doi.org/https://doi.org/10.48550/arXiv.1307.1091>

ВПЛИВ ТЕМПЕРАТУРИ ПІДКЛАДКИ НА МОРФОЛОГІЮ ТА КРИСТАЛІЧНІСТЬ ТОНКИХ ПЛІВОК TiO₂, ВИРОЩЕНИХ МЕТОДОМ ALD З ВИКОРИСТАННЯМ TTIP ТА H₂O

Темур К. Турдалієв, Ходжіахмат Х. Зохідов, Шухрат Ч. Іскандаров, Усмонджон Ф. Бердієв

Інститут іонно-плазмових та лазерних технологій ім. Аріфова Академії наук Узбекистану

100125, вул. Дурмон йулі, 33, Ташкент, Узбекистан

У цьому дослідженні досліджується вплив температури підкладки на морфологічні та структурні характеристики тонких плівок TiO₂, синтезованих методом термічного ALD з використанням тетраізопропоксиду титану та води як прекурсорів. Температура підкладки змінювалася від 200 до 275°C з кроком 25°C. Морфологію поверхні досліджували за допомогою атомно-силової мікроскопії, а кристалічну структуру аналізували за допомогою рентгенівської дифракції та раманівської спектроскопії. Було виявлено, що плівки, нанесені при 200°C, мали аморфну структуру та гладку, конформну поверхню з мінімальною шорсткістю. Підвищення температури до 225°C призвело до утворення мікроструктур та появи початкових ознак кристалізації, що супроводжувалося збільшенням шорсткості поверхні. При 250-275°C утворилася чітко виражена полікристалічна структура анатазу, що характеризується розвитком зерен та агломерацією наноструктур, про що свідчить підвищена інтенсивність дифракційних піків та вищі параметри шорсткості поверхні. Згідно з рентгенівським дифракційним аналізом, середній розмір кристалітів коливався від 32 до 71 нм, залежно від температури синтезу. Результати показують, що температура осадження має комплексний вплив як на фазовий склад, так і на морфологію поверхні плівок TiO₂, що необхідно враховувати для їх застосування у функціональних наноструктурах, фотокаталітичних системах, сенсорах та мікроелектронних пристроях.

Ключові слова: TiO₂; ALD; анатаз; кристалічність; морфологія; температура підкладки; XRD; раманівська спектроскопія